SERIAL NO. SSC-59

First

PROGRESS REPORT

(Project SR-108)

on

CRITICAL STRESS FOR SLIP, TWINNING, AND CLEAVAGE IN SINGLE CRYSTALS OF IRON

by

J. J. Cox, Jr., G. T. Horne and R. F. Mehl
CARNEGIE INSTITUTE OF TECHNOLOGY

Transmitted through

NATIONAL RESEARCH COUNCIL'S
COMMITTEE ON SHIP STEEL

Advisory to

SHIP STRUCTURE COMMITTEE

Division of Engineering and Industrial Research
National Academy of Sciences - National Research Council
Washington, D. C.

May 15, 1953

SSC-59

First
PROGRESS REPORT
(Project SR-108)

on

CRITICAL STRESS FOR SLIP, TWINNING, AND CLEAVAGE IN SINGLE CRYSTALS OF IRON

by

J. J. Cox, Jr.
G. T. Horne
R. F. Mehl

CARNEGIE INSTITUTE OF TECHNOLOGY
METALS RESEARCH LABORATORY

under

Department of the Navy
Bureau of Ships Contract NObs-50230
BuShips Project No. NS-011-080

for

SHIP STRUCTURE COMMITTEE

TABLE OF CONTENTS

LIST OF FIGURES

CRITICAL STRESS FOR SLIP, TWINNING, AND CLEAVAGE IN SINGLE CRYSTALS OF IRON

Introduction

Whether the low temperature brittleness of steel and the brittle fracture characteristics of ship plate can be correlated with a true ductile-to-brittle transition in pure iron has long been a question in the minds of engineers and metallurgists. If such a correlation exists, can the transition phenomenon be eliminated or raised by heat treatment or alloying additions? This and other questions can only be answered by experiments that examine the modes of deformation in single crystals.

A survey of existing literature reveals many experimental studies of deformation of single crystals of hexagonal and face-centered-cubic metals. Zinc, cadmium, aluminum, copper, and alpha brass have been studied extensively, and values of the shear stress required to initiate slip and twinning have been obtained at various temperatures for the several metals. The traces of the glide or twin planes upon the polished surface of the specimens were used to determine the crystallographic plane of deformation. These traces were lines which outlined one or more sets of low index planes and directions. In the hexagonal metals, the glide plane was the (0001) and the glide direction the $[2\bar{1}\bar{1}0]$. The face-centered

metals and alloys exhibited glide planes of the (111) type and $[10\bar{1}]$ directions--again the plane of highest atom density and the closest packed direction. Some variation in the glide plane occurred with changes in temperature, state of stress, and manner of loading; but in all cases the direction of closest packing was operative.

If the body-centered lattices were to deform in a similar manner, the predicted glide plane should be the (110) and the direction the [111]. However, metallographic specimens of α-iron deformed in compression at room temperature showed forked and wavy slip lines which indicated no single crystallographic plane. This initial observation led to several investigations on the mechanism of deformation in alpha iron.

In 1926 Taylor and Elam[1] tested small single crystals of relatively pure ferrite in both tension and compression. A rectangular grid work was engraved on the polished surface of the specimens, and the subsequent change in shape of the rectangles upon deformation enabled the investigators to calculate the plane and direction of slip. They concluded that the glide plane either coincided with or lay near the plane of maximum shear stress containing the [111] direction. Since the pole of the glide plane sometimes fell between two planes of low index, the authors proposed a theory of non-crystallographic or "banal" glide. Taylor and Elam also

considered multiple slip on non-parallel planes containing the [111] direction, thus giving a wavy effect to the slip lines but discarded this explanation in favor of the banal mechanism.

In 1928 Taylor[2] continued his work on the body-centered-cubic structure using beta brass and observed that the results were quite similar. One exception, however, seemed significant. In iron, when the pole of the glide plane did not coincide with a low index plane, it was always inclined away from the maximum shear stress pole toward the nearest (112) plane containing the slip direction; but in beta brass, the glide plane poles were always inclined toward the nearest (110) pole. On the basis of his observations, Taylor derived an equation relating the resistance to shear of a given plane to its position in the (111) zone:

$$F = \frac{P}{A} \cos\xi \quad \sin\xi \quad \cos(X - \Psi).$$

where F = shear resistance

A = area of specimen

P = yield point load

ξ = angle between slip direction and specimen axis

X = angle between maximum shear plane and closest (110) plane (both containing the slip direction)

ψ = angle between slip plane and closest (110) pole.

By differentiation, and integration between the limits 0 and ψ, a relationship was obtained which enabled Taylor to calculate the ratio of the resistance to shear of any plane in the zone to

the resistance to shear of the (110) plane. Since this calculation produced a curve of resistance to shear versus ψ similar to that predicted by the banal mechanism, Taylor was convinced that this was correct. It does not seem likely that the body-centered lattice should differ so radically in its deforming characteristics from all other lattices.

Some four years later, Fahrenhorst and Schmid[3], in Germany, studied the plastic flow of iron crystals by more or less indirect observation. They obtained orientation measurements of their crystals but used no grids and measured no glide traces. Instead, they assumed that there were four possible planes on which slip could occur:

1. On the (110) plane
2. On the (123) plane
3. On the (112) plane
4. On the maximum shear stress plane.

They concluded that the systems (123): [111] explained the observations. Measurements of shear stress and shear strain strengthened their belief in this mechanism since the scatter or variation in results was less for this system than for the others.

These conclusions are not necessarily correct for the variation in the data; assuming any of the four systems to operate leads to results which are equal within the limits of experimental errors.

However significant the conclusions, this work produced a simple method for the determination of the slip direction from the migration of the specimen axis during deformation. Two or more Laue photograms are taken at successive stages in the extension or compression of the crystal and the stereographic projections of these pictures are superimposed. A line drawn through the load axes at the different stages intersects the pole of the slip direction. A few exceptions were found, but in general the slip direction was [111] .

Barrett, Ansel, and Mehl[4], of this laboratory, examined the deformation mechanisms of single crystals of iron and silicon ferrite at several temperatures using sheet specimens of single crystal material. The trace normal method described by Barrett[5] was used to determine the slip plane and in every instance the glide plane could be explained by one of the planes (110), (112), or (123) within the limits of accuracy of the method. Since it was implicitly assumed that slip was crystallographic in the [111] zone, the results are not so conclusive as one might be led to believe.

Twinning and cleavage were also studied in this investigation. The twin system was found to be (112): [111] and the cleavage plane the (100). In the alloyed crystals, increasing the silicon content tended to:

1. Increase the temperature at which twinning occurred.
2. Increase the frequency of slip on the (110) [111] system.
3. Decrease the waviness of the slip lines.

Schematic curves of critical resolved shear stress for slip and twinning and critical normal stress for cleavage as a function of temperature were plotted (see Fig. 1).

Andrade[6] stated that the testing temperature determines the operative glide plane and on this basis calculated ratios of test temperature to melting point for several metals. This criterion is not adequate except for the alkali metals since several slip planes are found on a single specimen. Smoluchowski[7] proposed that the ionic core repulsion in non-alkali metals may qualitatively account for their deviation from the Andrade relationships.

Opinsky and Smoluchowski[8,9] stated that the slip system is determined by the position of the specimen in the unit stereographic triangle, as shown in Fig. 2. These areas or regions are calculated assuming that the shearing strength of the (110), (112), and (123) planes are equal. The authors pointed out that this may not be true but that there are no data upon which to base a different approach. Again it is implicitly assumed that the glide ellipse is both macroscopically and microscopically a true atomic plane.

Chen and Maddin[10] explored the nature of slip in single crystal wires of molybdenum and found the pole of the glide ellipse to vary along the [111] zone. Their picture was one of cooperative slip on planes of the (110) type. Segments of varying length of two (110) planes could form slip lines with poles

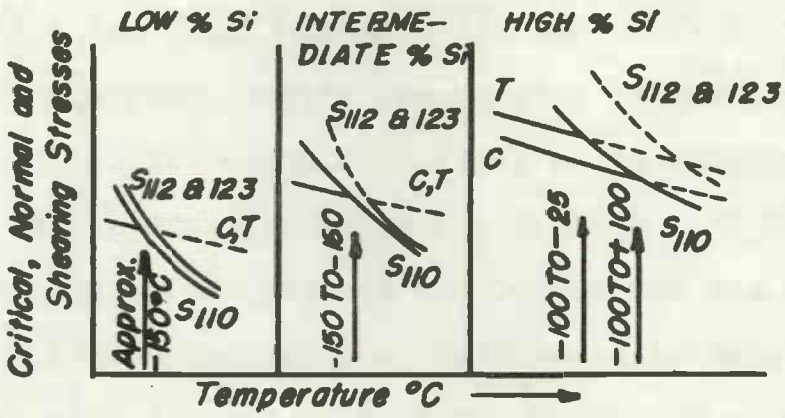

Fig. 1

Critical Resolved Shear Stress versus Temperature. (After Barrett, Ansel and Mehl)

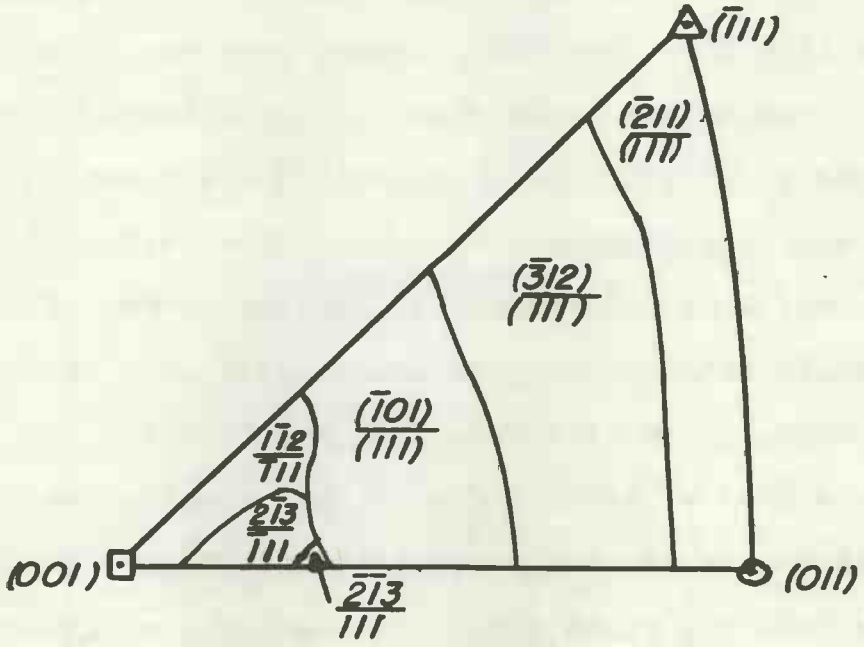

Fig. 2

Regions of highest resolved shear stress in the unit stereographic triangle. (After Opinsky and Smoluchowski)

lying anywhere along the [111] zone. Brick and Vogel[11], in the discussion to this paper, suggest that when the pole of the integrated glide ellipse coincides with a (110) pole, the trace of this ellipse should be straight at any azimuthal position on the surface of the specimen. If, perhaps, cooperative slip on (112) or (123) was the mechanism, then this is not a valid objection. Maddin points out also that lattice rotation could account for this behavior.

The data of all investigators appear to be quite similar, but the explanations differ quite markedly. It is true that a mechanism involving high index planes does not seem plausible, for the shearing strengths of these planes are expected to be quite high; yet the experimental results indicate that the wavy slip lines are not in every case explained by cooperative shear on low index planes. The failure of all proposed mechanisms to explain the observations are related in a common fault--insufficient resolving power. The real need in any case is for a new tool to detect the plane or planes of slip on an atomic scale rather than on a microscopic one. Our techniques are too crude by several orders of magnitude.

The method of attack of this investigation was to measure the glide traces of single crystals and resolve the stress at yielding onto the glide plane. The super-complex nature of slip in iron was not anticipated as causing trouble in a stress measuring experiment within the accuracies required, and

consequently a tangential course into the realm of deformation mechanistics was not plotted. However, since the work of Brick and Vogel and Chen and Maddin, plus the early results of this project, have indicated the importance of resolving the complex nature of slip in iron, the original plans have been somewhat modified. The objectives of this investigation reported herein are as follows:

1. To produce a ferrite of nominal purity from SAE 1008 steel.
2. To grow single crystals of this material of a size suitable for subsequent tension tests.
3. To find the critical resolved shear stresses for slip and twinning insofar as they can be determined as a function of temperature.
4. To determine whether a transistion from slip to twinning occurs with repoducibility of results and whether a criterion for the onset of twinning can be established.
5. To study the fracture properties of single crystals as a function of temperature, strain, aging, and prestrain.
6. To investigate the atomic nature of slip in iron by methods of higher resolving power, e.g.,
    a. The electron microscope.
    b. Multiple beam interferometry.

7. To correlate the above in a general theory of deformation for α-iron.

Experimental Techniques

The ideal material for producing single crystals of relatively pure iron would be a vacuum melted high purity iron such as Westinghouse "Puron" or National Research Corporation pure iron. Preliminary experiments failed to produce a successful strain anneal cycle for single crystal production. Several shapes and sizes of specimens were tried but with little or no success. It was believed that the variation in properties of the irons from batch to batch prevented the data from one heat of iron being applicable to another heat.

Alternate possibilities were Armco iron, such as that used by Stone[12], or decarburized SAE 1008 steel after Gensamer[13]. The decarburized steel was chosen for its cleanliness as compared with the Armco iron, although the total soluble impurities were much higher. The analysis of the steel was as follows:

C	Si	Mn	P	S	Cr	Ti	Mo	Ni	Cu
0.09	0.14	0.46	0.010	0.027	0.08	0.01	0.01	0.07	0.05

Twelve tensile bars were machined to the specifications shown in Fig. 3. The radius of curvature at the shoulder is

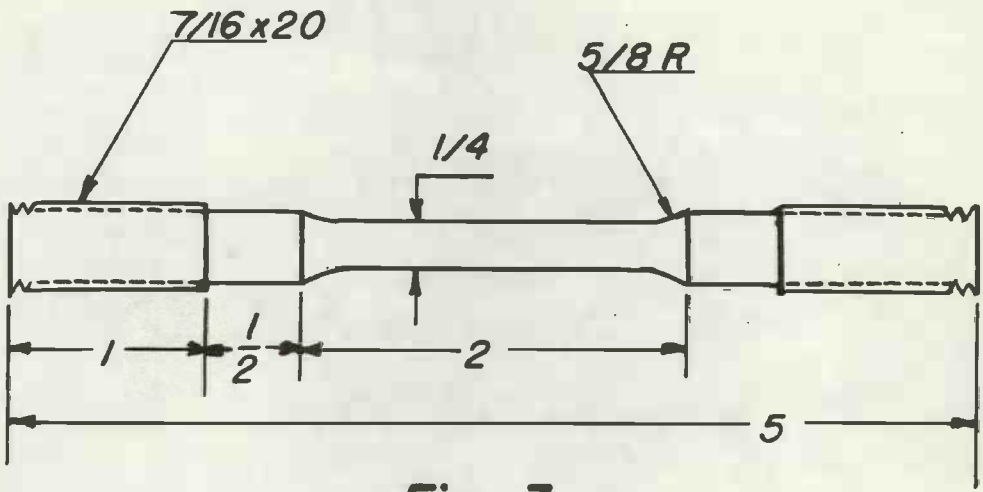

Fig. 3

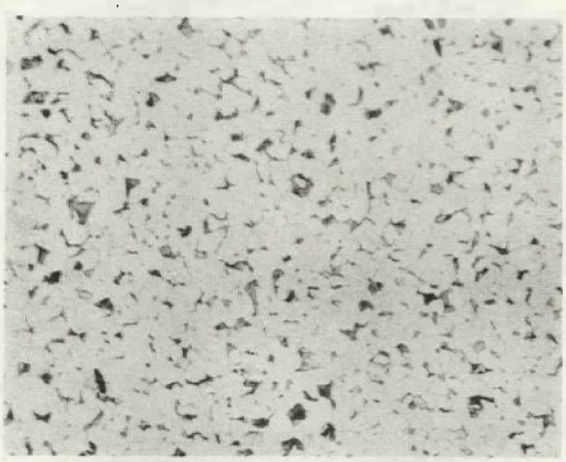

S.A.E. 1008 Bar Stock as Received

Fig. 4

Fig. 5. Columnar crystals radiating from the edge of a specimen partially decarburized in the region of the phase diagram. (X10)

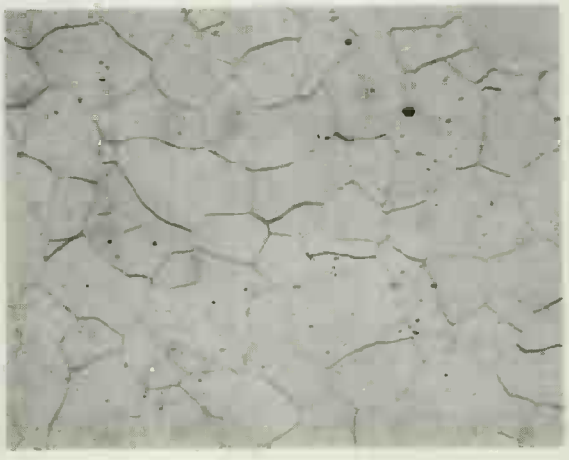

Fig. 6. Decarburized S.A.E. 1008 stock (X100)

not shown but was 5/8 in. They were decarburized for 100 hrs. at 720°C in hydrogen saturated with water vapor at 68°C. The controller allowed the furnace to overshoot above 730°C, and the specimens were decarburized in the ($\alpha + \gamma$) phase field resulting in a structure of columnar grains projecting from the outside to the center of the specimens. It was realized that the diffusion coefficient of carbon in α-iron at 720°C is four times as great as that of carbon in γ-iron at 1000°C,

$$1000°C \quad D_{\gamma}^{c} = 2.42 \times 10^{-7} \text{ sq. cm. per sec.}$$
$$720°C \quad D_{\alpha}^{c} = 9.25 \times 10^{-7} \text{ sq. cm. per sec.}$$

but the fluctuation in line voltages at night were too unpredictable to permit accurate control of furnace temperature. Therefore, the temperature of 950°C was chosen as the decarburizing temperature.

The structure of the mild steel in as-received condition is shown in Fig.4 . The grain size is ASTM #8-9. For strain anneal methods, the grain size should be much larger since the critical strain increases with increasing grain size. Considering both treatments, grain growth anneal and decarburization, the 950°C treatment seemed most suitable.

It was found necessary to heat the specimens under a very dry H_2 atmosphere to prevent the formation of columnar crystals while passing through the $\alpha+\gamma$ phase region. An example of this is shown in Fig. 5. Another reason for heating and cooling without

water saturation, is that the degree of saturation used is calculated on the basis of the iron-oxygen equilibrium at 950°C; consequently, this H_2/H_2O ratio is in equilibrium with FeO at temperatures below about 920°C and produces an oxidized surface.

The grain size was controlled by inserting a small resistance in series with the furnace at the end of the soak period. This is sufficient to decrease the current-temperature equilibrium of the furnace to about 850°C, thus giving the correct cooling rate through the α to γ transformation to produce a grain size of ASTM #2-3. The structure of the final decarburized material is shown in Fig. 6. The composition of the decarburized material was identical with that shown earlier for the bar stock, with the exception that the carbon content was reduced to 0.019%.

A series of twelve decarburized specimens were strained from 2.0% to 4.4% elongation in a one-inch gauge length in increments of 0.2%. The specimens were placed in a furnace under a dry hydrogen atomsphere and heated rapidly to 350°C. The furnace was then program-heated at 5°F per hr. to the soak temperature of 880°C, annealed for 4 days, then furnace cooled to room temperature.

Upon removal from the furnace, the specimens were observed to have a heat etched surface showing a grain size of about ASTM #000. They were then milled longitudinally to half

diameter, polished through #000 metallographic paper and etched in a 10% nital solution. The results are shown in Fig. 7.

It can be seen from Fig. 7 that the critical strain was about 3.2%. This value was chosen, and all subsequent specimens were strained 3.2% and subjected to a similar treatment. The yield has been about 50 per cent single crystals, the remainder being almost exclusively bi-crystals, with one or two tri-crystals. Milling the specimens would, of course, ruin them for further testing, so a procedure was developed for detecting the "single-crystalness" of the treated specimens. Upon removal from the growth anneal, the specimens were electropolished and etched repeatedly until a structure different from the false surface structure became apparent. Specimens showing a single crystal extending from one shoulder of the specimen to the other were electropolished and etched until no "grain islands" appeared on the surface, then given a final polish to prepare the surface for optical and X-ray examination.

Brick and Vogel[11] used an 880°C anneal in purified helium subsequent to a metallographic polish to produce a suitable surface. The present authors tried this but discarded it in favor of the electropolish method when it was found that the annealing treatment gave the same undistorted

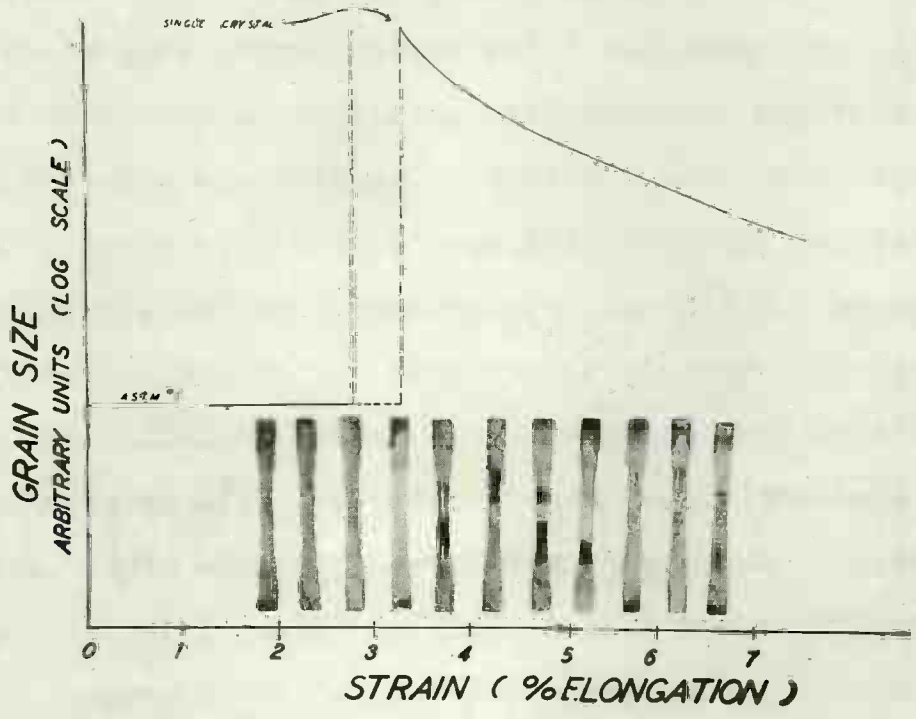

Fig. 7. Results of experiments to determine the critical deformation to produce single crystals of decarburized S.A.E. 1008

of the anneal method is to lower the inclusion loss from the surface. Electrolytic methods create galvanic attack at the metal-inclusion interface which make the inclusions "pop out" during polishing. This was not believed to be of serious consequence in the type of measurements to be made, and since the electropolishing is much easier, it was used in all subsequent preparations.

The orientation of all specimens was determined by Laue back-reflection methods using tungsten radiation. Sharp clear spots were obtained in all cases, thereby confirming the unstressed nature of the surface.

The tensile tests were performed on a Dillon chain driven tensile machine of 5,000 lbs. capacity. The load was measured with a Baldwin-Southwark type U-1, SR-4, load cell exciting the input circuit of a Sanborn strain gauge amplifier and recorder. This system produces a record of load versus time.

The strain was measured by means of a specially constructed strain gauge employing two linear differential transformers which are connected to a parallel compensated Schaevitz recorder. This apparatus records elongation versus time. It would have been most desirable to have an X-Y recorder with one axis load and the other strain, but unfortunately, this piece of equipment

sufficient to show the yield point in most crystals, although autographic load-elongation curves would be much better.

An insulated container surrounded the specimens at all temperatures and contained the various media used to obtain the test temperature. The cooling media are listed below:

+200°C	- Russian mineral oil
+100°C	- Boiling water
Room Temp.	- Stagnant air
0°C	- Ice + water mixture
-70°C	- Dry ice + acetone mixture
-196°C	- Liquid nitrogen

The specimens were protected by a coating of rubber cement to prevent scratching and corrosion by the temperature medium. This coating was easily stripped off after testing and retained the electropolished surface very well.

Measurements of the traces of slip and twin markings were made on a special goniometer head similar to that described by Brick and Vogel[11]. This goniometer is the same one used to align the specimen for the Laue pictures and prevents errors in angular measurement when the specimen is transferred from one goniometer to another. The goniometer was attached to the rotating head of a Bausch

and Lomb research metallograph and locked in position by a thumb screw. Measurements of the angle of inclination of the glide plane to the specimen axis were made at 10°- intervals around the specimen.

The angular measurements were plotted stereographically and were found to fall on a great circle with errors less than 4 to 5 degrees in the worst cases. The pole of this great circle was the pole of the particular glide plane. In all cases the over-all orientation of the glide ellipse was measured and hereinafter will be called the integrated glide ellipse.

Experimental Results

Geometrically the problem of determining a critical resolved shear stress consists very simply of obtaining a yield stress and resolving it into a given plane in space--the space being the specimen itself. The complexities arise from the experimental determinations of the yield stress, the plane of glide or twinning or cleavage, and the direction lying in that plane.

The Slip Plane

Figs. 8 to 20 show the orientations of all crystals referred to the standard (001) projection, while Fig. 21 summarizes the relative positions of the maximum shear

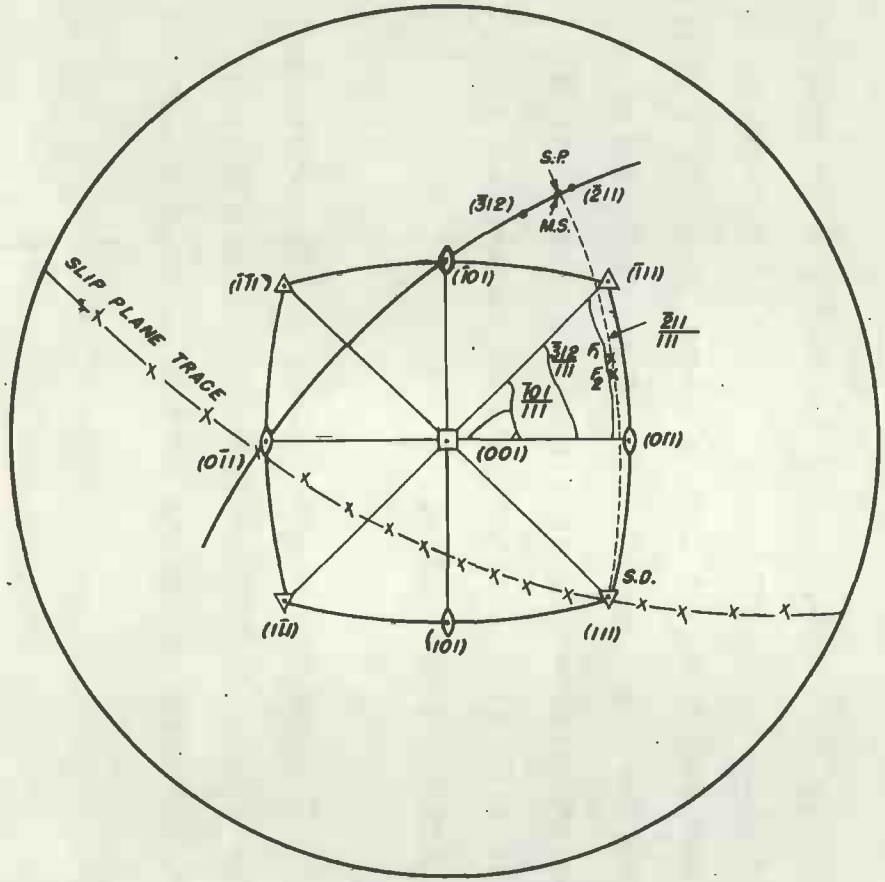

Projection of Specimen Br-2

$F_1 F_2$ Specimen Axis Before and After Deformation

M.S. Pole of Maximum Shear Plane Containing (111)

S.P. Pole of Slip Plane

S.D. Slip Direction

Fig. 8

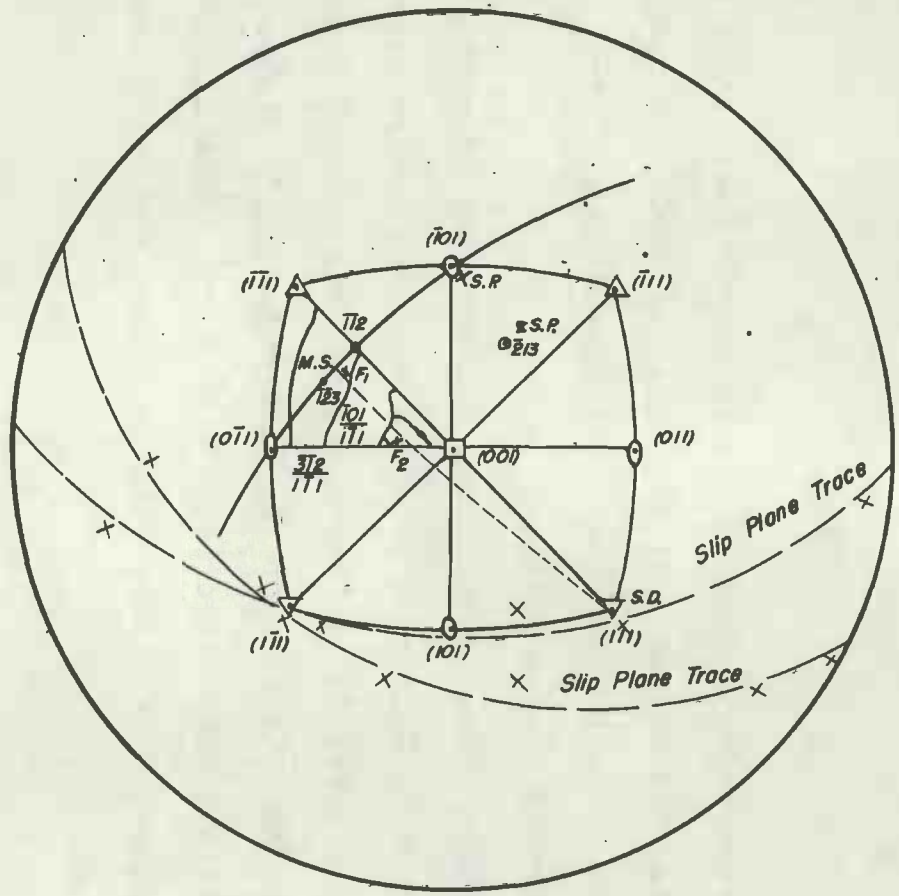

Projection of Specimen A-7

$F_1 F_2$ Specimen Axis Before and After Deformation.

M.S. Pole of Maximum Shear Plane Containing (111)

S.P. Pole of Slip Plane

S.D. Slip Direction

Fig. 9

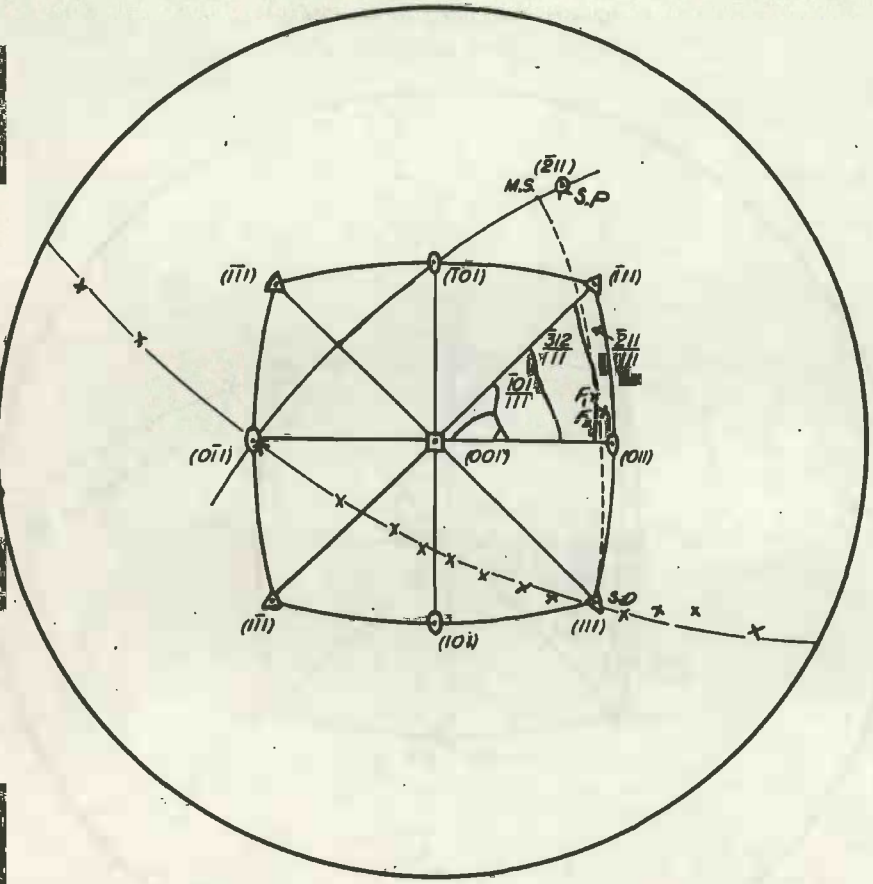

Projection of Specimen A-1

Fi, Fe	Specimen Axis Before and After Deformation
M.S.	Pole of Maximum Shear Plane Containing (111)
S.P.	Pole of Slip Plane
S.D.	Slip Direction

Fig. 10

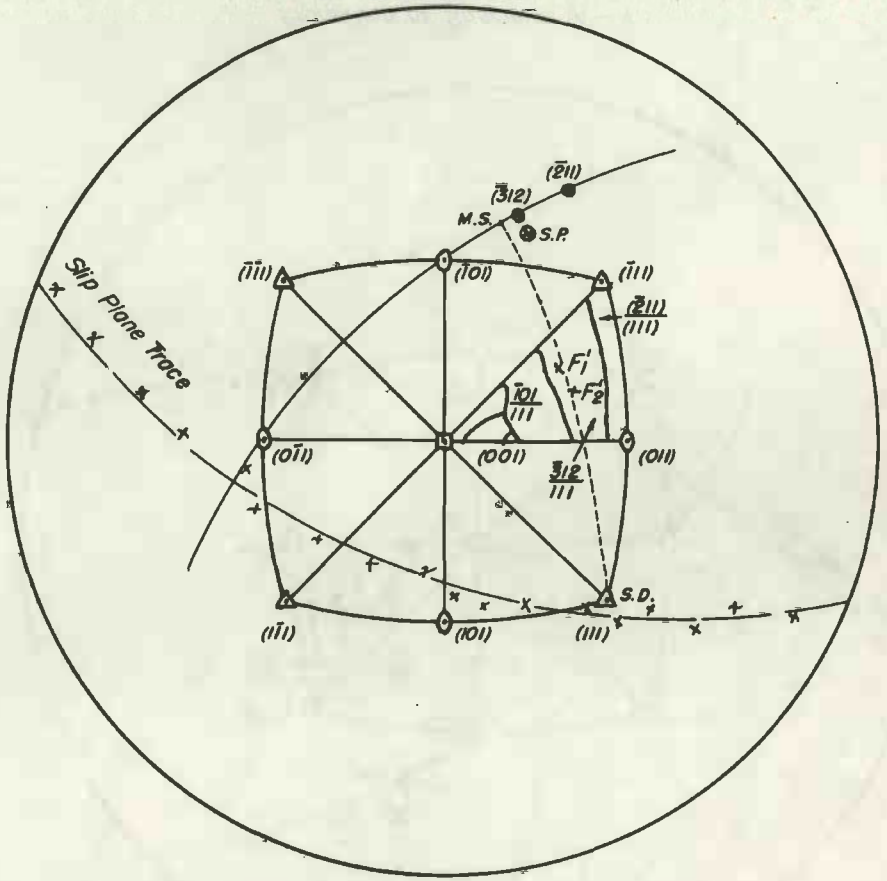

Projection of Specimen A-3

F_1', F_2'	Specimen Axis Before and After Deformation.
M.S.	Pole of Maximum Shear Plane Containing (111).
S.P.	Pole of Slip Plane.
S.D.	Slip Direction.

Fig. 11

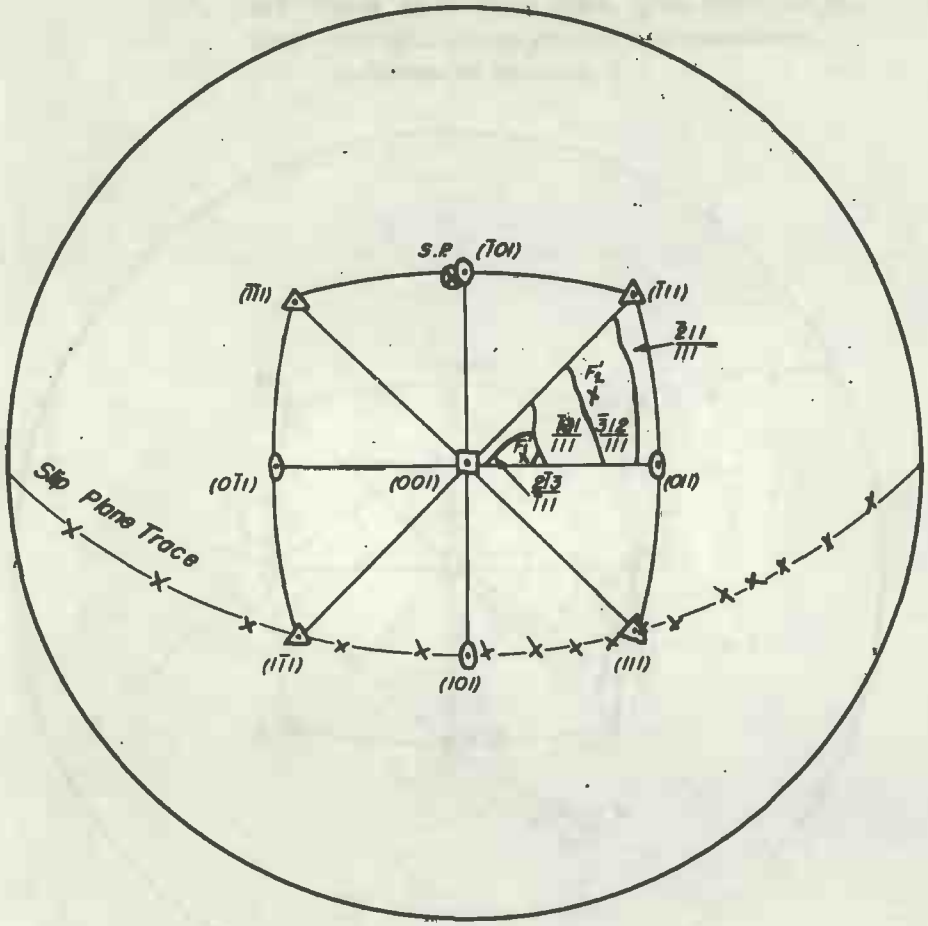

Projection of Specimen A— 5

F_1', F_2' Specimen Axis Before and After Deformation.
M.S. Pole of Maximum Shear Plane Containing (111).
S.P. Pole of Slip Plane.
S.D. Slip Direction.

Fig. 12

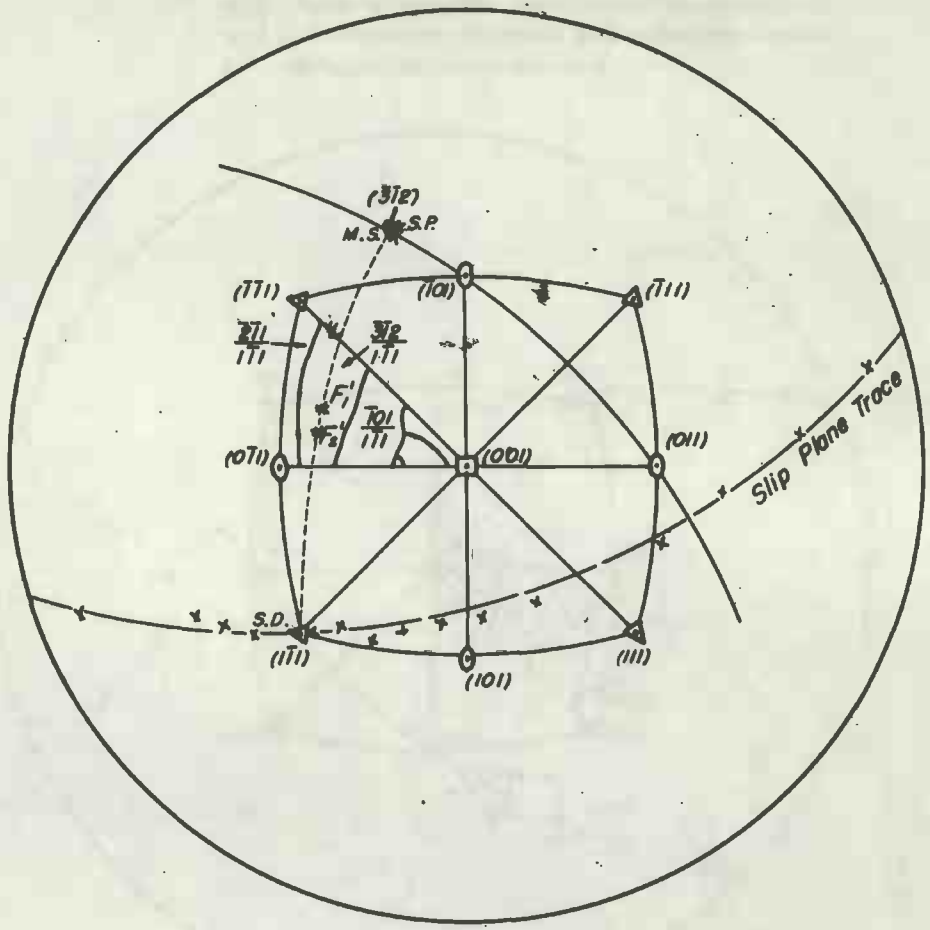

Projection of Specimen A — 4

F_1', F_2' Specimen Axis Before and After Deformation.
M.S. Pole of Maximum Shear Plane Containing (111).
S.P. Pole of Slip Plane.
S.D. Slip Direction.

Fig. 13

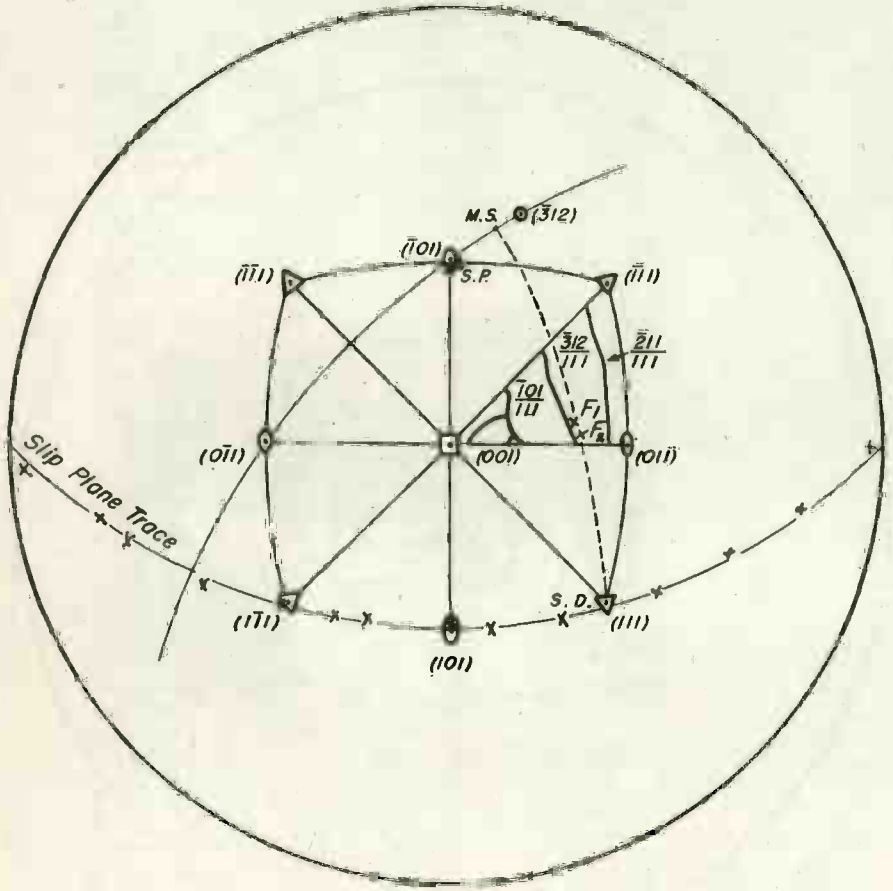

Projection of Specimen A-12

F_1F_2 Specimen Axis Before and After Deformation.

M.S. Pole of Maximum Shear Plane Containing (111)

S.P. Pole of Slip Plane.

S.D. Slip Direction.

Fig. 14

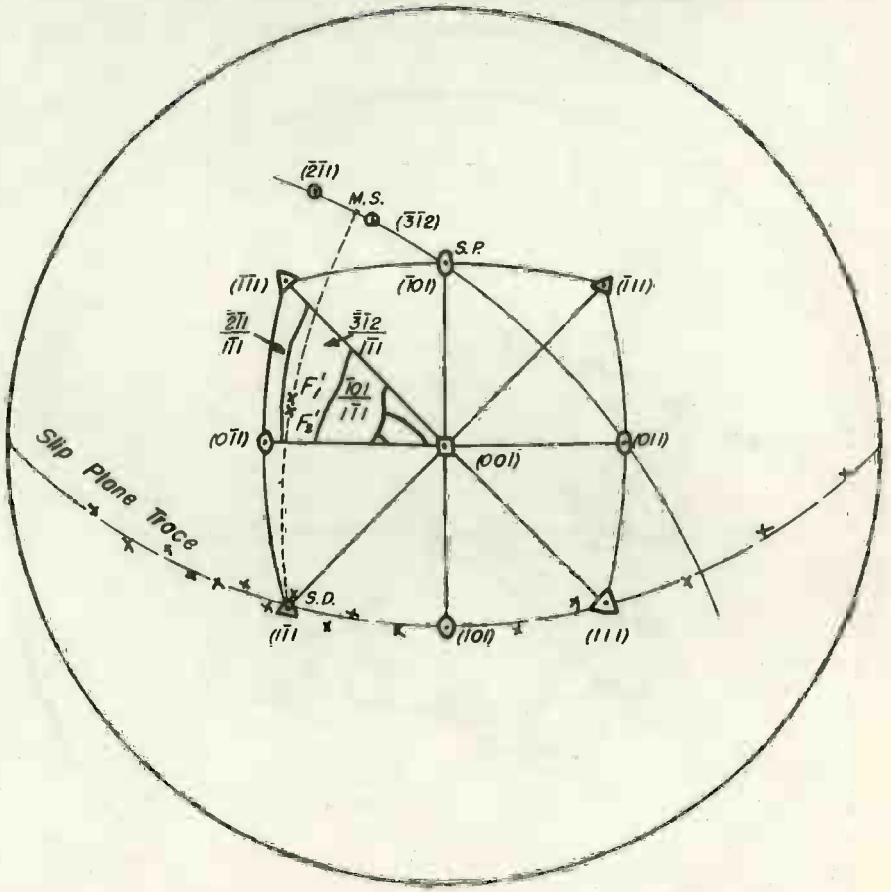

Projection of Specimen A-6

$F_1'F_2'$ Specimen Axis Before and After Deformation

M.S. Pole of Maximum Shear Plane Containing (111)

S.P. Pole of Slip Plane

S.D. Slip Direction

Fig. 15

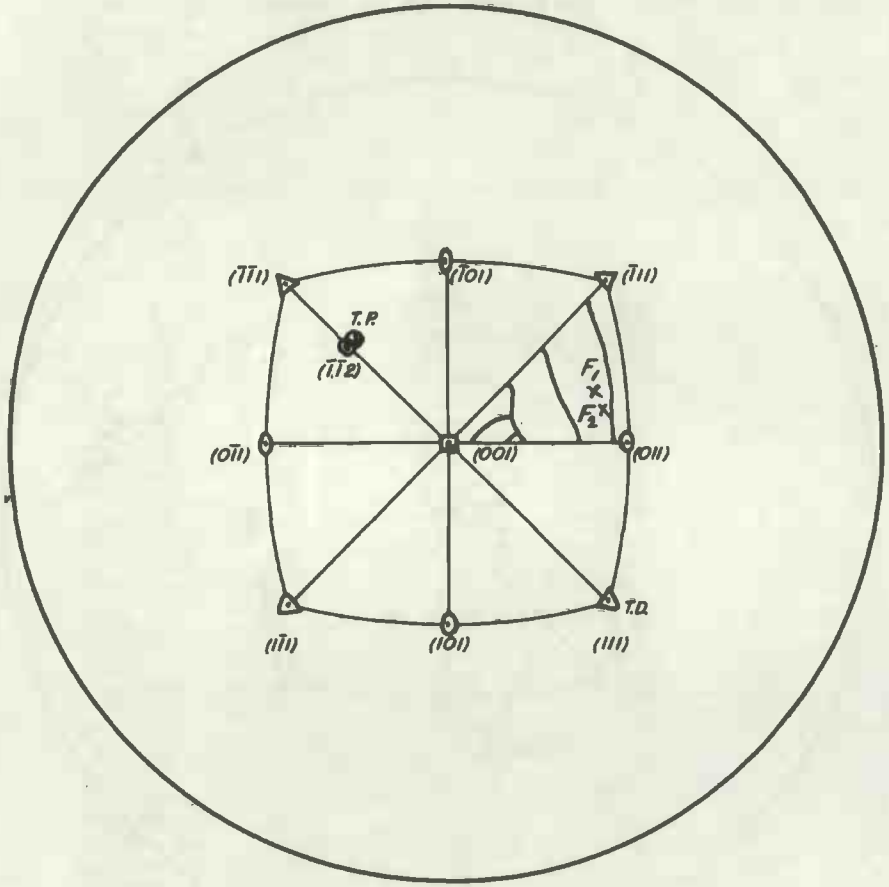

Projection of Specimen A-6

$F_1 F_2$ Specimen Axis Before and After Deformation
T.P. Pole of Twin Plane
T.D. Twin Direction

Fig. 16

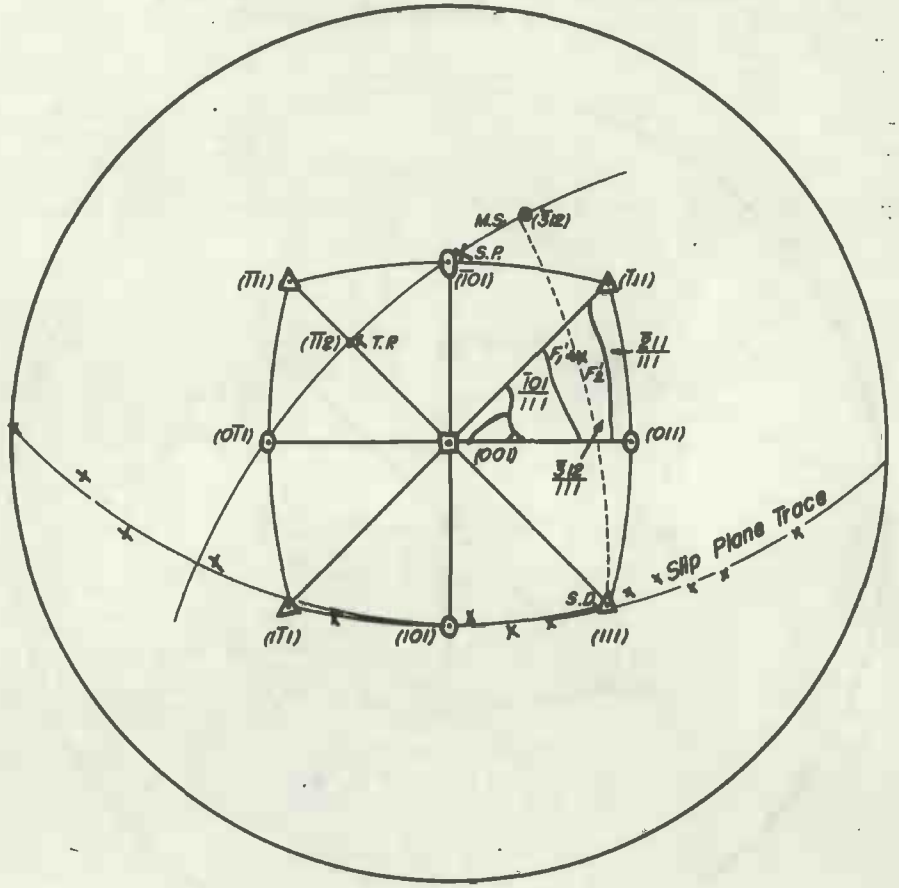

Projection of Specimen A-9

$F_1' F_2'$ Specimen Axis Before and After Deformation.
M.S. Pole of Maximum Shear Plane Containing (111).
S.P. Pole of Slip Plane.
S.D. Slip Direction
T.P. Pole of Twin Plane

Fig. 17

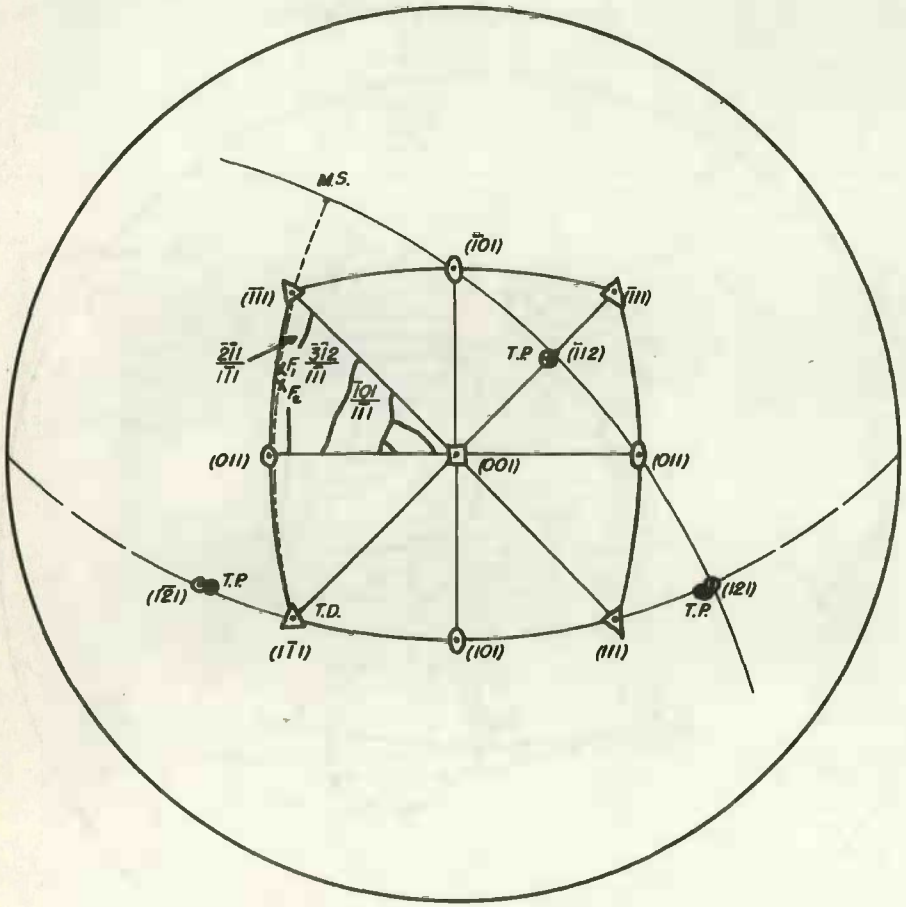

Projection of Specimen A-11

F_1, F_2 Specimen Axis Before and After Deformation.
M.S. Pole of Maximum Shear Plane Containing (111)
T.P. Pole of Twin Plane.
T.D. Twin Direction.

Fig. 18

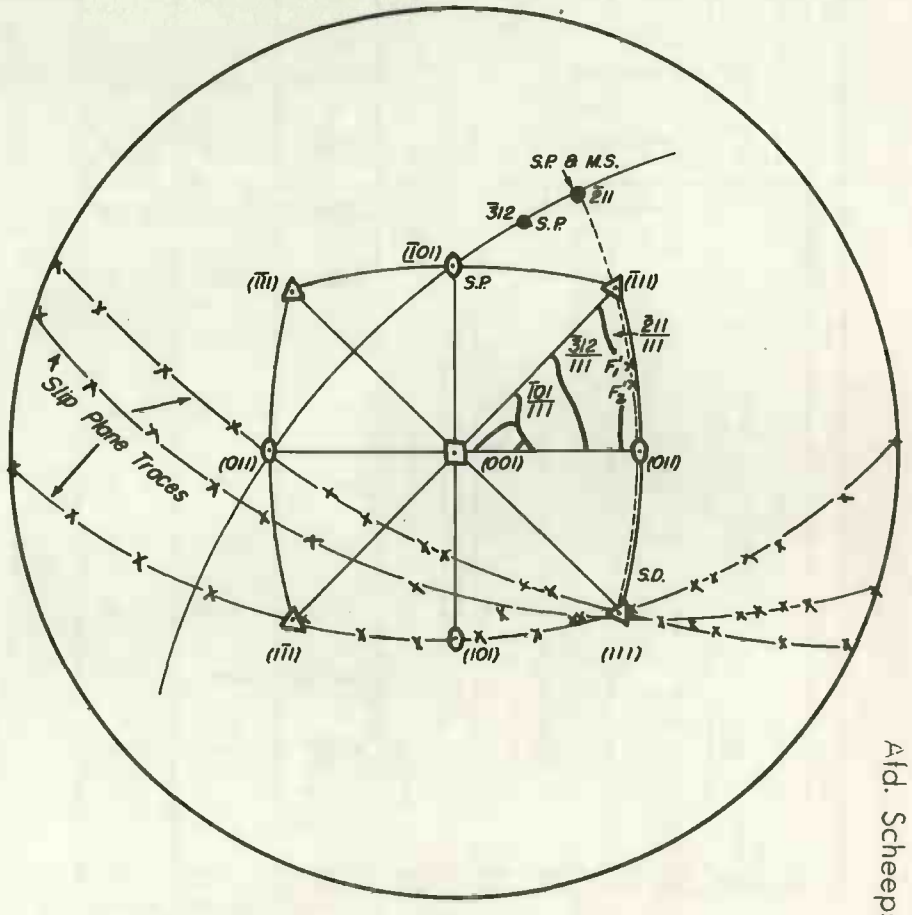

Projection of Specimen A-11

$F_1'F_2'$ Specimen Axis Before and After Deformation
M.S. Pole of Maximum Shear Plane Containing (111)
S.P. Pole of Slip Plane
S.D. Slip Direction.

Fig. 19

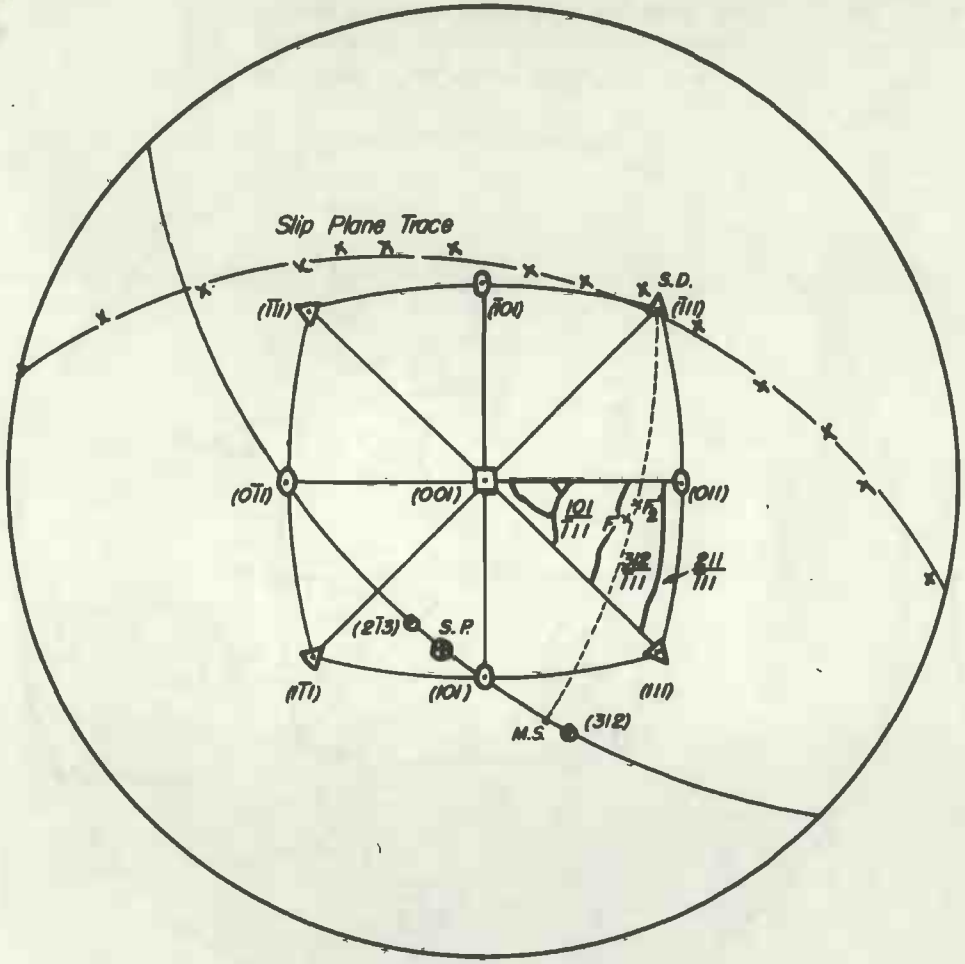

Projection of Specimen Br-3

$F_1'F_2'$ Specimen Axis Before and After Deformation.
M.S. Pole of Maximum Shear Plane Containing (111).
S.P. Pole of Slip Plane.
S.D. Slip Direction.

Fig. 20

Relative Positions of Maximum Shear Stress Poles (•) and Glide Plane Poles (x).

Specimen Number	Slip Direction	Temperature °C
Br-2	(111)	+195°
A-7	—	+98°
Br-3	(1̄11)	+25°
A-1	(111)	+31°
A-3	(111)	0°
A-5	(1̄11) & (111)	0°
A-4	(11̄1)	-73°
A-12	(111)	-70°
A-6	(11̄1)	-196°
A-9	(111)	-196°
A-11	(111)	-196°

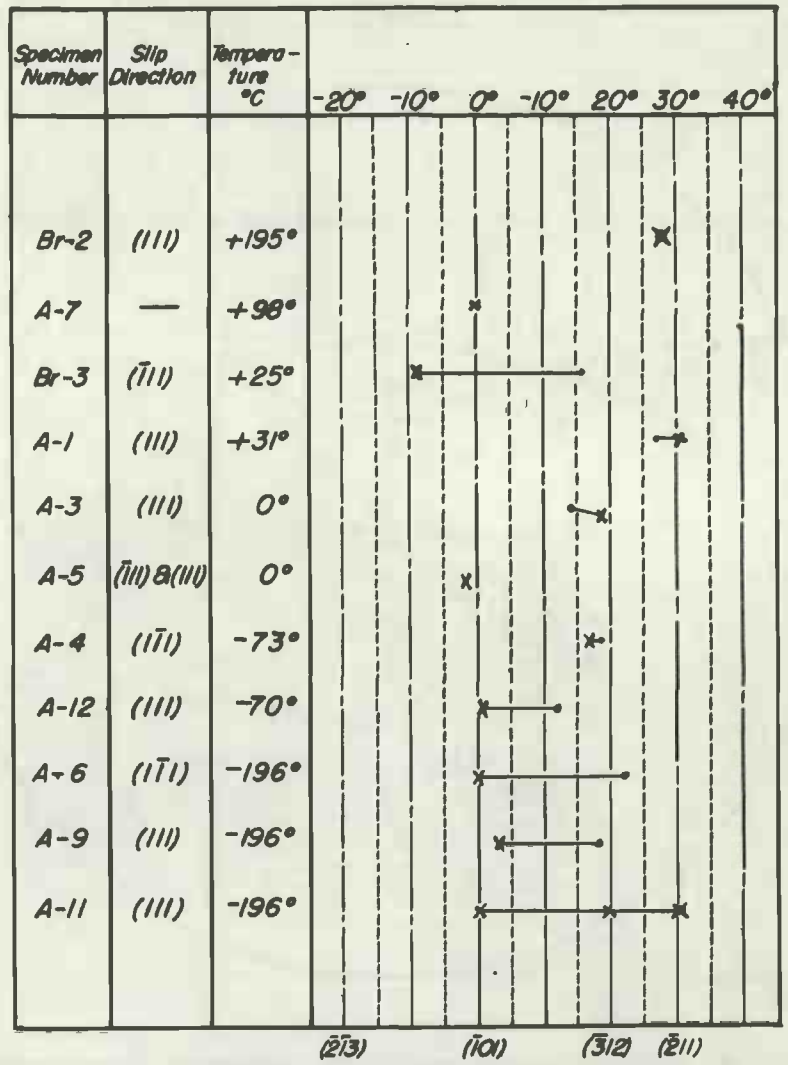

Fig. 21

stress planes and the glide planes for all the specimens. The plane of maximum shear stress is determined stereographically by drawing a great circle through the poles of the specimen axis (F_1, F_2) to the point where it intersects the [111] zone. This intersection (MS) is the pole of the maximum shear stress plane. This great circle is terminated on the other end by the slip direction (SD).

From Fig. 21, it can be seen that at low temperatures the slip plane is always inclined toward and usually coincides with the $(\bar{1}01)$ plane. In specimen A-11 three sets of planes were visible; however, the $(\bar{1}01)$ plane was most prominent. At higher temperatures it appears that the glide plane is inclined toward the nearest low index plane (110), (112), or (123). No maximum shear stress plane is indicated for specimens A-7 and A-5 because the slip direction is not clearly indicated. Specimen BR-3 does not follow either trend and cannot be accounted for at the present time. In all cases, except that of BR-3, the pole of the integrated glide ellipse lies close enough to either a (110), (112), or (123) plane to be considered as having that orientation.

The Slip Direction

The method of Fahrenhorst and Schmid was used to determine the slip direction--that of extrapolating the great circle drawn through the poles of the specimen axis before

and after deformation. In eight of the ten specimens, the slip direction was clearly the [111] . Specimens A-5 and A-7 gave complex results, but they are to be expected when the specimens are located near two possible slip planes not having a common slip direction.

The Yield Point

Sharp inhomogeneous yield phenomena were not observed in all specimens although the analyses showed 0.012% carbon to be present. Figs. 26 to 35 show the load-time curves for each crystal. The scale of load is not indicated on each chart, for it varies with adjustment of the sensitivity of the recorder; but each curve is referred to a standard calibration chart and the load computed from there. Specimens A-12, A-1, A-3, BR-3, and A-4 show what might be called double yielding. At least there is a leveling off of the curve after the initial change in slope.

Specimens A-11, A-9, and A-6 were strained at -196°C and exhibited twinning as the principal mode of deformation. There is no change in slope of the load-time curve for such a case but merely a sudden drop in load accompanied by a loud "bang" followed by an increase in load parallel to the original curve before twinning. The large breaks in the curves are caused by a change in scale of the recording apparatus. Although the strain was measured over the entire reduced section of the test bar, no cases could be found where the strain

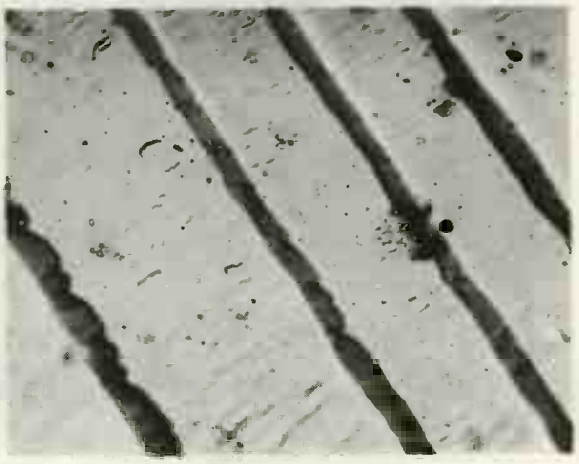

Fig. 22a. Twins and slip lines in specimen A-11 (X1000)

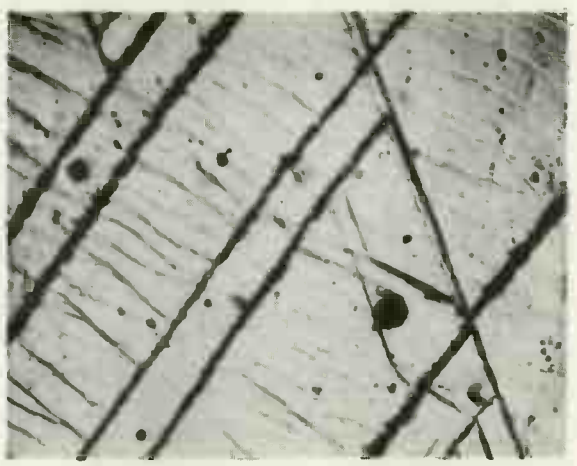

Fig. 22b. Twins and slip lines in specimen A-11 (X150)

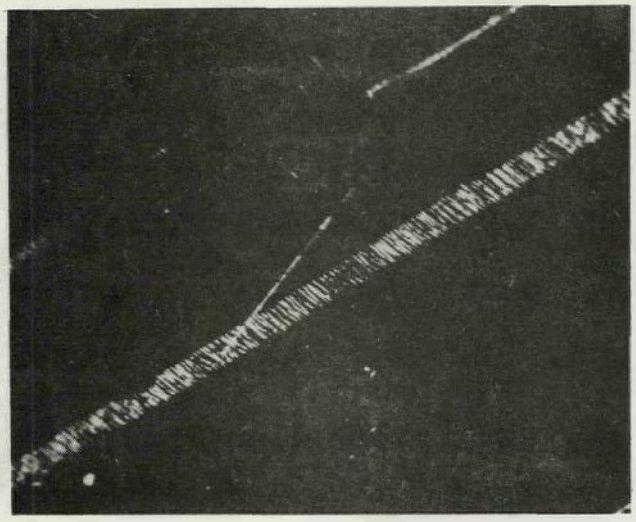

Fig. 23. Slip lines appearing in scratch parallel to compression axis of single crystal (X 150) Polarized Light.

Fig. 24. Same as Fig. 23 but vertical illumination (X 1000)

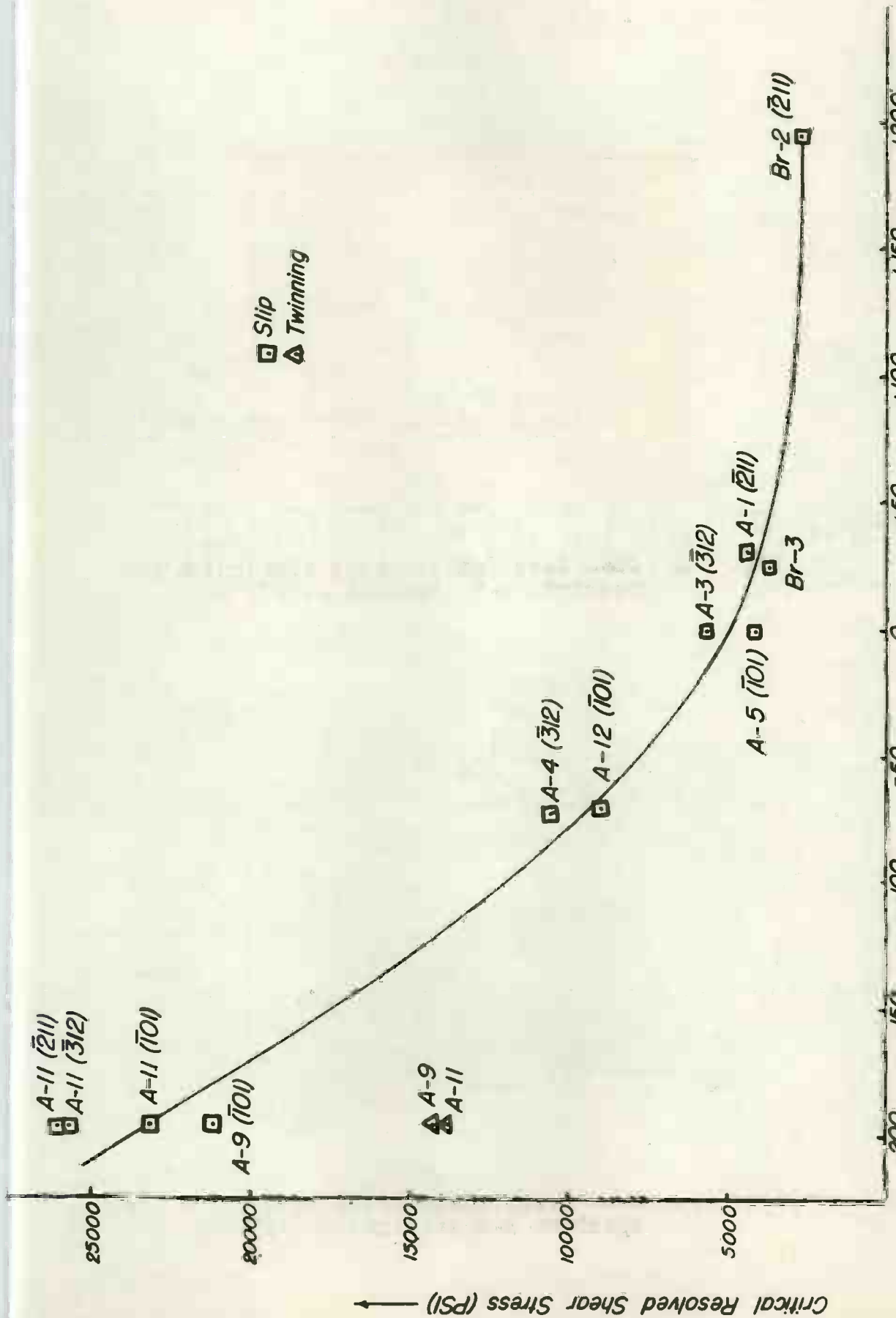
Critical Resolved Shear Stress (PSI)
25000
20000
15000
10000
5000
-200
-150
-100
-50
0
+50
+100
+150
+200
Temperature °C
A-11 (2̄11)
A-11 (3̄12)
A-11 (1̄01)
A-9 (1̄01)
A-9
A-11
A-4 (3̄12)
A-12 (1̄01)
A-3 (3̄12)
A-5 (1̄01)
A-1 (2̄11)
Br-3
Br-2 (2̄11)
Slip
Twinning

Fig. 25

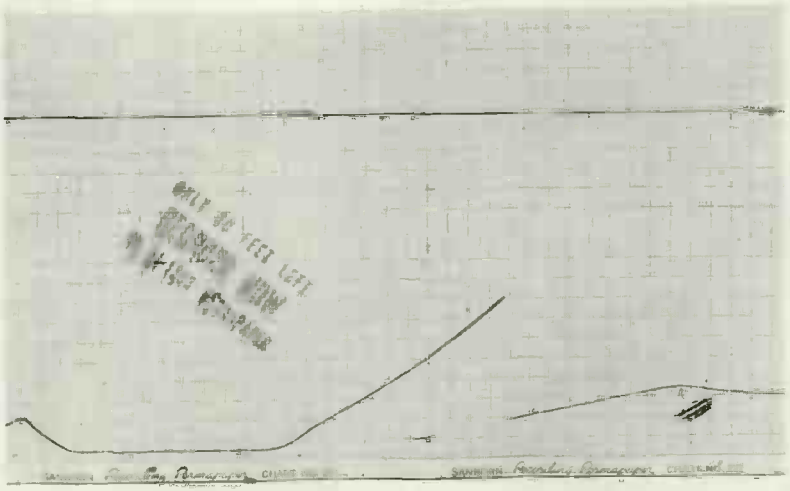

Fig. 26. Load (vertical) versus time curve for specimen A-4 strained at -73°C.

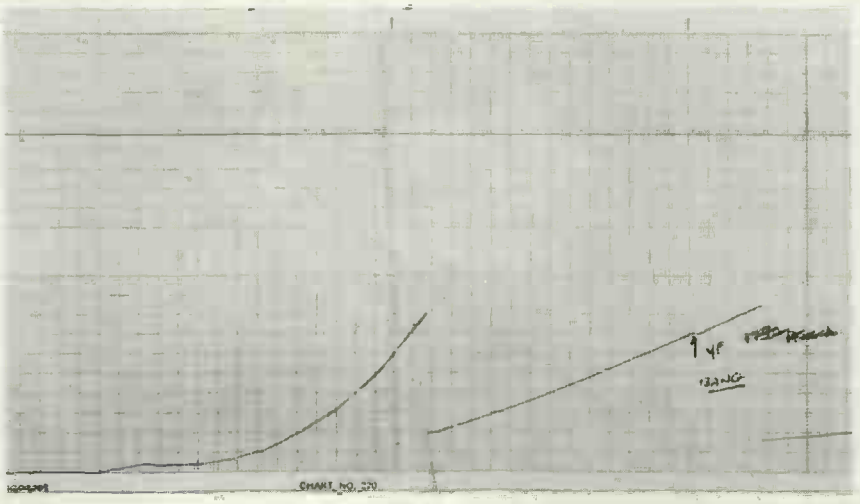

Fig. 27. Load (vertical) versus time curve for specimen A-6 strained at -196°C.

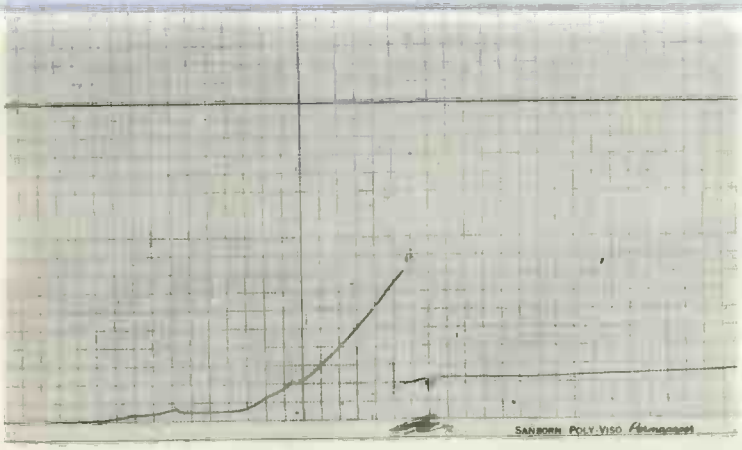

Fig. 28. Load (vertical) versus time curve for specimen Br-3 strained at 25°C.

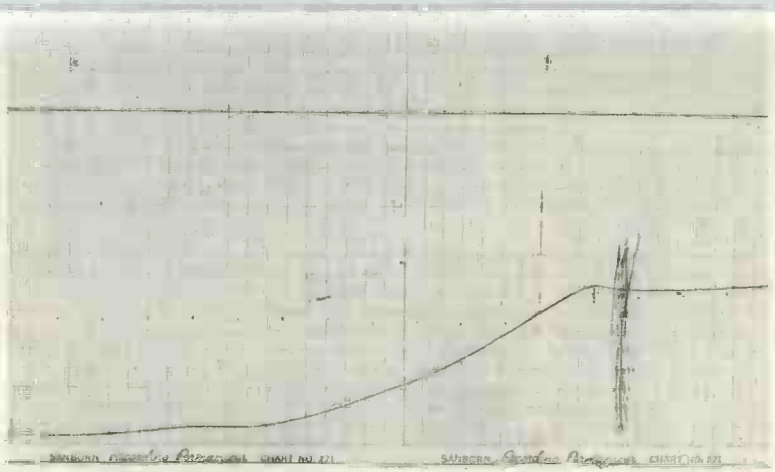

Fig. 29. Load (vertical) versus time curve for specimen A-3 strained at 0°C.

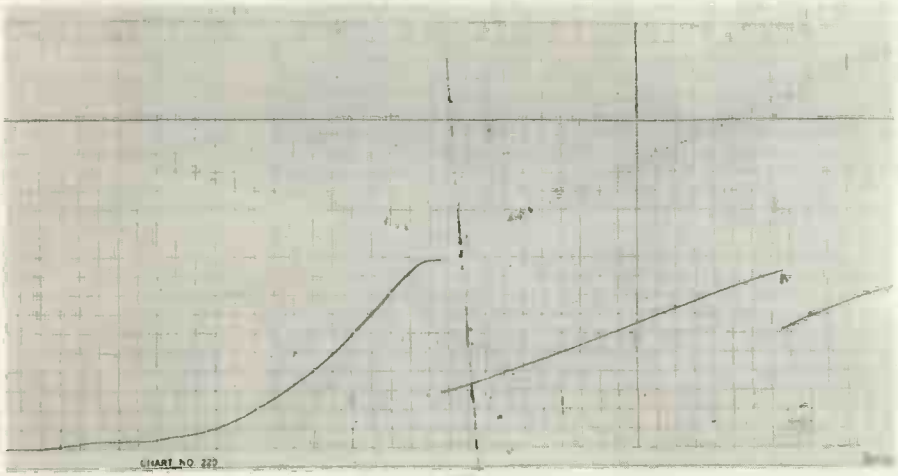

Fig. 30. Load (ordinate) versus time curve for specimen A-9 strained at -196°C.

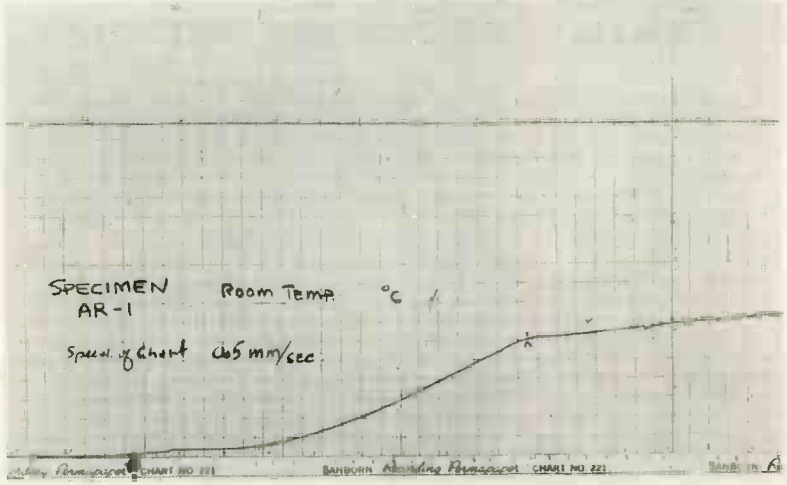

Fig. 31. Load (ordinate) versus time curve for specimen A-1 strained at 31°C.

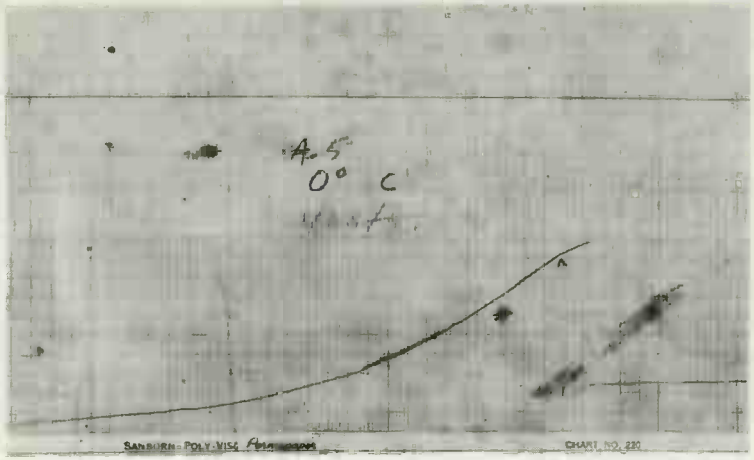

Fig. 32. Load (vertical) versus time curve for specimen A-5 strained at 0°C.

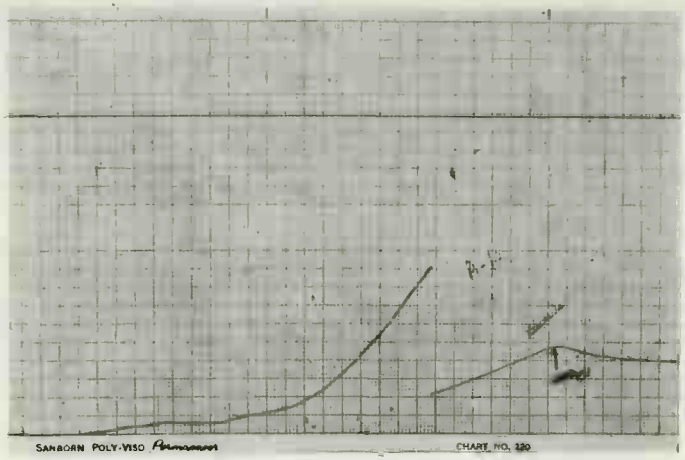

Fig. 33. Load (vertical) versus time curve for specimen A-12 strained at -70°C.

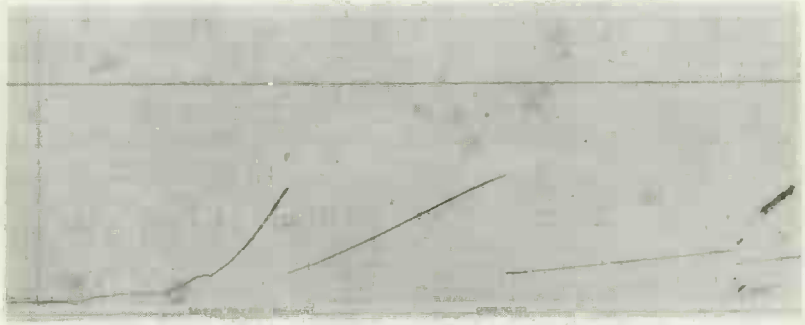

Fig. 34. Load (ordinate) versus time curve for specimen A-11 strained at -196°C.

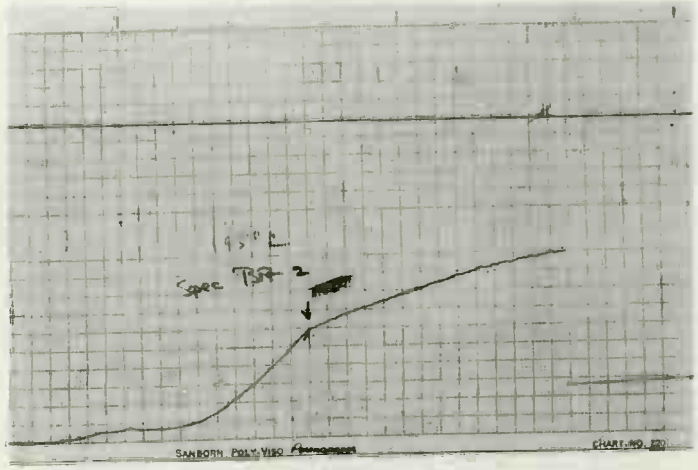

Fig. 35. Load (ordinate) versus time curve for specimen Br-2 strained at 195°C.

occurred preferentially along the crystal. Something resembling Lüders bands were observed on the specimens pulled at room temperature and 0°C, but the strains were not high enough to permit definite conclusions to be made concerning this.

The Nature of Slip and Twin Traces

The most difficult part of this investigation is the observation and measurement of the traces of the glide or twin planes. At low deformations such as 2-4%, the slip lines appear as very faint striations on the surface and can only be seen at certain magnifications and under certain lighting conditions. This is particularly true for specimens tested between -70°C and +30°C. At higher or lower temperatures, they seem to be more visible. As in previous investigation the slip lines were found to vary in linearity and forkedness with position relative to the slip direction.

When in one specimen it was observed that slip lines were much more visible in a scratch on the specimen, a special single crystal was deliberately scratched with a diamond and deformed in compression. The results are shown in Figs. 23 and 24. Within the scratch the lines are broad and distinct but are nowhere else visible. This is in agreement with Paxton et al.[14] that mechanical deformation of the surface increases the visibility of the lines and changes their appearance from a striated one to a series of discrete steps.

Electron Microscope and Interferometric Studies

No results from the electron microscopy studies are available at this time except to say that replicas of a smooth unstrained surface of the crystals have been satisfactorily prepared. It is hoped that very soon some results on the nature of the slip lines at high resolving powers will be forthcoming.

Preliminary experiments on the Tolansky interferometer indicates the height differences between the lines shown in Figs. 24 and 25 is approximately 300-500 $\mathring{A}$. The technique must be further refined before quantitative results will be available.

Critical Stresses for Slip and Twinning

Table I and Fig. 25 show the results of attempts to calculate the critical resolved shear stresses for slip and twinning. The scatter between duplicate specimens is quite small and well within the expected error. The constancy predicted by critical resolved shear stress law seems to be fairly well obeyed.

Critical stresses for twinning are recorded for two specimens, A-9 and A-11. These values are also quite similar. In these specimens, it was not possible to determine whether slip or twinning occurred initially since traces of both were found. Photomicrographs of specimen A-11 are shown in Figs. 22(a) and (b). An unmarked specimen tested at -196°C showed

Studiecentrum T. N. O.
Scheepsbouw en Navigatie
Afd. Scheepsbouw, DELFT

TABLE I

Specimen No.	Test Temp., °C	Slip Plane	Critical Resolved Shear Stress on Slip Plane	MSS Plane	(101)	(123)	(112)
BR-2	195	(211)	2735	2735	2432	2735	2735
A-7	98	(101)	--	--	--	--	--
BR-3	25	(?)	3786	4017	4017	4017	3941
A-1	31	(211)	4411	4411	4023	4411	4336
A-3	0	(312)	5676	5484	5414	5484	5275
A-5	0	(101)	4146	--	4146	--	--
A-4	73	(312) (110)	10570	10570	10070	10570	10410
A-12	70	(101)	9000	9173	8825	9000	8646
A-6	196	(101)	17270	18530	17270	18530	18220
A-9	196	(101)	21200	21690	20690	21690	21200
A-11	196	(101) (312) (211)	23150 25800 26150	26150	23150	25800	26150

no slip lines when removed immediately after yielding.

Discussion

The position of the integrated glide ellipse in iron is found to follow two distinct patterns. At -70°C and below, the pole of the integrated ellipse coincides with a (110) pole regardless of the orientation of the crystal and the plane of maximum shear stress. Although traces of (112) and (123) planes appear at low temperatures, the (110) trace is most prominent. In each case, except that of BR-3, the pole of the glide ellipse lies close enough to one of the three low index planes of the [111] zone to say that the slip is crystallographic on a macroscopic or average basis. But does this have significance? In certain aspects, yes, in that it allows the stress on this integrated plane of glide to be calculated and a curve of critical stress for slip to be plotted as a function of temperature. Fundamentally, though, we are measuring the position of a nonentity. The integrated glide plane is a hypotetical one consisting of the best straight line than can be drawn through a series of forked and wavy lines. By definition it is not a plane.

On the other hand, the concept of the integrated ellipse is not altogether useless. It enables a rough

ketch of the deformation picture to be made from various ombinations of planes and directions. Essentially all the xperiments on deformation of single crystals of iron have evealed the same data that:

1. Slip line traces are forked and wavy and that the waviness varies with respect to the slip direction.
2. The position of the integrated glide ellipse may occupy any position in the [111] zone and may or may not coincide with the maximum shear stress plane.
3. Lower temperatures favor slip on the (110) type planes.
4. The twinning plane is definitely the (112).

ny of the proposed theories explain some of the observations ut not others. A theory of combined slip on various planes ould, with a little evasiveness of tongue, explain all the bservations. The problem remains to find a measuring stick apable of resolving the atomic nature of slip and then, start- ng from that point, to construct a theory of deformation for he body-centered-cubic lattice.

Twinning was predominant in specimens A-11, A-9, and A-6. t would be desirable to determine whether twinning occurred efore, after, or during slip; but so far this has not been ossible. If twinning occurs simultaneously with slip, this ill indeed be difficult to detect. Critical resolved shear

stress appears to be the criterion for twinning, but the data are not complete enough to make this conclusion a definite one.

Certain effects on the appearance of slip lines as affected by surface condition are found to be of interest. Mechanical deformation of the surface changes the markings from fine striations to coarse discrete lines which appear at much lower strains. This is in accord with the work of Paxton, who showed that mechanical polishing of a single crystal increased the visibility of slip lines as compared with those on an electropolished surface. The problem remains as to which of the two structures is the true one. One would suppose that the striated appearance of the electropolished and supposedly undeformed surface is the true effect, and yet this striated appearance is peculiar to the body-centered lattice. The markings found on mechanically polished surfaces or in scratches on electropolished surfaces are more like those found in metals of other crystal structures, although they are forked and wavy. When results are complete on the electron microscope and interferometric studies, perhaps more can be said concerning the effect of surface condition upon the nature of the slip markings.

Fig. 36 shows a Laue photogram after deformation. The phenomenon to be noted here is the separating of spots into three or four discrete layers. This is similar to observations made on polygonization in recrystallized metals and

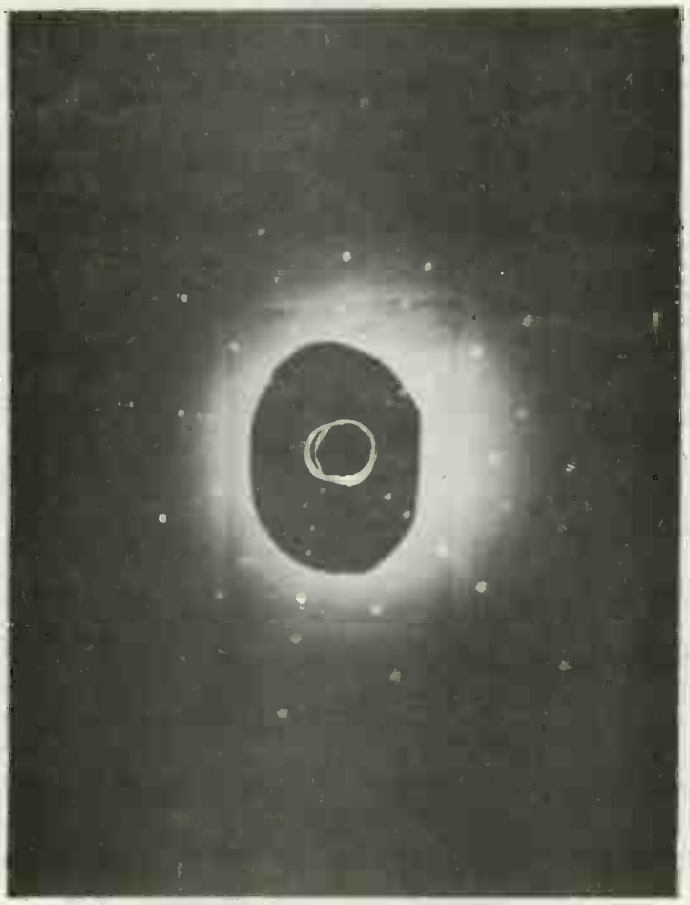

Fig. 36. Laue photogram of specimen A-1 after 4% strain, showing the splitting of spots.

may perhaps be due to a "polygonal" lattice of slight misfit caused by the deformation. This is pure speculation and the answer is not known, but it is included for curiosity's sake.

Future Work

The results obtained thus far in this investigation are perhaps too scant to confirm any one theory of slip or twinning. Further tensile data above -70°C should help to define the behavior of the integrated glide ellipse as a function of temperature and orientation but will probably not obtain insight into the deformation mechanism on an atomic scale. On the other hand, the electron microscope and interferometer may uncover some interesting points on the atomic or at least submicroscopic mechanism.

The other part of the program which needs investigation is that of the slip to twinning transition. Here the difficulties should be only experimental in nature. To obtain constant temperature baths in suitable intervals from -70°C to -196°C is a very difficult problem. Elaborate and expensive refrigeration systems are completely out of the question. Perhaps some cooling system involving liquid nitrogen circulating through coils immersed in a suitable liquid would be satisfactory.

The study of cleavage is even more difficult from an experimental standpoint. The three specimens tested at

-196°C have shown no cleavage and this was expected since no (001) planes were suitably oriented. In fact only two or three crystals have an orientation that places a (100) pole close to the specimen axis. Perhaps even in these specimens, cleavage will not occur at -196°C. If not, then the temperature must be drastically lowered to liquid hydrogen or liquid helium. Both of these coolants are not ideally suited since hydrogen is explosive and helium is almost prohibitively expensive.

There are then three possible places upon which to concentrate effort for the closing six months of this project:

1. Slip:

   Test several specimens of varying orientation between -70°C and +200°C with the hope of finding a regular variation to the behavior of the glide ellipse.

2. Twinning:

   a. Construct a suitable cooling apparatus to obtain temperatures from -70°C to -196°C.

   b. Test several specimens in this temperature range to determine (1) at what temperature twinning begins; (2) does slip precede, accompany, or follow twinning below the temperature found in (1); and (3) whether twinning can be correlated with a critical resolved shear stress theory.

3. Cleavage:

a. To obtain a cooling medium that will promote cleavage in any specimen regardless of orientation.

b. To calculate a fracture stress curve for single crystals of iron.

c. To verify the critical normal stress theory of cleavage for iron.

With each of these investigations, a concurrent study of the submicroscopic nature of slip would be carried out with specimens already strained; that is, no crystals would be "wasted" on such an investigation.

Bibliography

1. G. I. Taylor and C. F. Elam, Proceedings Royal Society of London, Volume A112, (1926), p. 337.

2. G. I. Taylor, Proceedings Royal Society of London, Volume A118, (1928), p. 1.

3. N. Fahrenhorst and E. Schmid, Zeitschrift für Physik, Volume 78, (1932), p. 383.

4. C. S. Barrett, G. Ansel, and R. F. Mehl, Trans. Amer. Soc. Metals, Volume 25, (1937), p. 702.

5. C. S. Barrett, Structure of Metals, McGraw-Hill, New York.

6. E. W. da. C. Andrade, Proceedings Physical Soc., Volume 52, (1940), p. 1.

7. R. Smoluchowski, Discussion to Chen and Maddin article, Journal of Metals, 1952.

8. A. J. Opinsky and R. Smoluchowski, Journal Applied Physics, Volume 22, (1951), p. 1428.

9. A. J. Opinsky and R. Smoluchowski, Doctorate Dissertation, Carnegie Institute of Technology, 1950.

10. N. K. Chen and R. Maddin, Trans. Amer. Inst. Mining & Met. Engrs., Volume 191, (1951), p. 937.

11. F. L. Vogel, Jr., and R. M. Brick, Univ. of Pennsylvania Technical Report #1 to Flight Research Lab., Wright-Patterson Air Force Base.

12. F. G. Stone, Trans. Amer. Inst. Mining and Met. Engrs., Volume 175, (1948), p. 908.

13. M. Gensamer and R. F. Mehl, Trans. Amer. Inst. Mining and Met. Engrs., Volume 131, (1938).

14. H. Paxton, Private communication. To be published, University of Birmingham, England.